Lateral-nonuniformity effect on the I-V spectrum in a double-barrier resonant-tunneling structure

Y. Fu and M. Willander
Department of Physics and Measurement Technology, Linköping University, S-58183 Linköping, Sweden
(Received 12 February 1991; revised manuscript received 10 April 1991)

The Schrödinger equation is solved self-consistently with the Poisson equation assuming coherent tunneling processes. The lateral-nonuniformity effect on the I-V spectrum is calculated in the double-barrier resonant-tunneling structure. Such an effect is attributed as a possible mechanism to explain the appearance of the fine structures adjacent to the principal tunneling peak in experimental I-V spectra. The lateral nonuniformity also substantially decreases the peak-to-valley ratio. The calculation indicates that this lateral nonuniformity effect can be reduced by increasing the well width, but as the energy width of the resonant state is also decreased, the tunneling current density is decreased. Therefore, the proper design of the device greatly depends on its application.

The fundamental characteristics of resonant tunneling are qualitatively well understood. Ricco and Azbel[1] showed that the resonant enhancement of the transmission coefficient occurs when the incident electron energy coincides with the energy of the bottom of the subband in the well, while it is pointed out[2,3] that the negative differential resistance can be solely explained as an electron transmission from the three-dimensional (3D) states in the emitter to the 3D states in the collector via the two-dimensional resonant states in the well. Self-consistent models have been published to include the space-charge regions formed in the biased double-barrier resonant-tunneling structure (DBRTS) within the Fabry-Pérot resonator[4] and the sequential-tunneling picture.[5] The intrinsic bistability in DBRTS is qualitatively explained by the charge accumulation in the quantum-well region.[6-8]

In this work we report the lateral nonuniformity effect on the I-V spectrum in DBRTS. By lateral nonuniformity we mean that, as the consequences of the surface kinetic processes, at the interface between two binary materials, such as AlAs/GaAs, a certain degree of both vertical and lateral intermixings of the two materials is inevitable. If the average terrace widths of the essential Ga- and Al-like regions at the intended interface are larger than a length scale on which the notion of bands is meaningful, then a well-defined value of the band-edge discontinuity at a well-defined spatial area exists. Such intermixing is clearly indicated by the fine-structure emission lines in the photoluminescence spectra corresponding well to that calculated for a ± 1-monolayer (ML) change in the well width.[9]

The double-barrier structure in this work is[6] n^+ $\langle 100 \rangle$ GaAs substrate and a 56-Å GaAs well sandwiched between two 85-Å $Al_{0.4}Ga_{0.6}As$ barriers. The GaAs emitter and collector (each 0.5 μm thick) have net donor concentrations about 2×10^{17} cm^{-3}.

The effective-mass approximation is used in the following theoretical calculation. The effective mass of the electron in $Al_xGa_{1-x}As$ assumes the commonly used value $m=(0.067+0.083x)m_0$, where m_0 is the vacuum electron mass. The conduction-band offset between GaAs well and $Al_xGa_{1-x}As$ barrier is $V=0.65\times(1.247x)$ eV, where 0.65 is the $Al_xGa_{1-x}As$ conduction-band–valence-band offset ratio and $1.247x$ eV comes from the relation between the $Al_xGa_{1-x}As$ band gap and the Al composition x: $E_g(Al_xGa_{1-x}As)=E_g(GaAs)+1.247x$ eV.[10] The conduction-band structure of DBRTS at steady state (thermal equilibrium without bias or steady current under bias) is described by the Schrödinger equation and the Poisson equation (the z direction is set as the growth direction):

$$\left[-\frac{\hbar^2}{2m}\frac{\partial^2}{\partial z^2}+E_c\right]\Psi=E\Psi\ , \tag{1}$$

$$\nabla(\epsilon\nabla U)=e\left[N-\sum_{E_c}^{\infty}f(E)|\Psi(E)|^2\right]\ , \tag{2}$$

where $E_c=V+eU$, N is the doping concentration,

$$f(E)=(mkT/\pi\hbar^2)\ln(e^{(E_f-E)/kT}+1)$$

is the electron occupation at state $\Psi(E)$, and $\epsilon=13.18-3.12x$ is the dielectric constant.[11]

The calculation is divided into two steps, one for the conduction-band structure and the other for the current density. The conduction-band structure is calculated in the following way to include charge-accumulation effects. The envelope wave function Ψ is separated into three coherent parts: (a) from the middle of the emitter barrier (the barrier connected with the emitter) to the region deep inside the emitter, (b) from the middle of the emitter barrier to the middle of collector barrier, and (c) from the middle of the collector barrier to the region deep inside the collector. Far away from the barrier plus well region, Ψ is in the form of a running wave, while at the middle of the barriers, we set $\Psi=0$. Ψ and $(1/m)(\partial\Psi/\partial z)$ are continuous in the three separate regions. The Poisson equation is solved as a boundary value problem: $U=E_{fe}$ (emitter far away from the barrier plus well region) and $U=E_{fc}$ (collector far away from the barrier plus well region). In the following text, "emitter or collector far away from the double-barrier region" is abbreviated as

"emitter or collector." E_{fe} and E_{fc} are obtained by assuming that the emitter and collector are independent bulk semiconductors at thermal equilibrium. With such boundary conditions, the Fermi level at thermal equilibrium is set at energy 0, as shown in Fig. 1. When the sample is biased, the quasi-Fermi levels of emitter and collector are no longer aligned at the same energy level but $E_{fe}-E_{fc}=eV_{ex}$, V_{ex} is the external applied voltage. Since it is the emitter that supplies the carriers to the electronic resonant states between the two barriers, the quasi-Fermi level of those resonant states is assumed to be E_{fe}. In Fig. 1 the band diagrams with 0.1- and 0.2-V bias are also plotted setting $E_{fe}=0$.

At thermal equilibrium, since the barrier plus well region is very thin, there is virtually no band bending at interfaces because of the doping concentration difference. The E_f is 18 meV above the conduction-band bottom in the electrodes far away from the barrier plus well region (donor concentration 2×10^{17} cm^{-3}). There is quite a thick depletion layer in the region of collector close to the collector barrier from our calculation when the applied voltage is large.

The current density is calculated using the above-obtained conduction-band structure. Two coordinates are defined: $z=0$ where the electrons start tunneling processes into the barrier plus well region and $z=L$ where the electrons are collected. The exact geometric positions of $z=0$ and L in the sample are influenced by doping levels in the electrodes and the external voltage.

Equation (1) is solved to obtain the transmission coefficient $T(E)$ between $z=0$ and L by the usual standard transfer matrix method. The tunneling current density is calculated by the following equation assuming parabolic conduction band and the conservation of momentum in the xy plane:

$$I=\frac{mekT}{2\hbar^3\pi^2}\int_{E_c(0)}^{\infty}de\,T(E)\ln\left[\frac{e^{[E_f(0)-E]/kT}+1}{e^{[E_f(L)-E]/kT}+1}\right], \quad (3)$$

where $E_f(i)$ is the quasi-Fermi level at $z=i$ and $i=0,L$.

A crucial factor in the I-V quantitative calculation is the proper determination of $z=0$ and L. Since the electron mean free path is very short in the heavily doped electrodes due to large impurity scattering rate, the electron wave functions in the emitter and collector are not coherent with each other, they are coherent only around the barrier plus well region with low impurity concentration. It is these coherent wave functions which are proper to use in the tunneling transmission calculation. In our calculation, $z=0$ is set at the place with the first carrier density peak closest to the emitter barrier. Since the choice of $z=L$ has a very small effect on the current density calculation when $E_{ce}>E_{fc}$ ($V_{ex}>18$ meV in the present sample), it is set at the symmetric position of $z=0$ in the collector region. The $z=0$ is chosen to ensure a largest tunneling current density. Both $z=0$ and L are indicated in Fig. 1 in our calculation.

The calculation assumes two monolayer changes in the barriers and well. For a (001) $Al_xGa_{1-x}As$ lattice, the distance between two adjacent atomic planes is 2.73 Å, and a two-monolayer change here is assumed to account for the simultaneous change of an anion layer and a cation one. Thus for GaAs/$Al_xGa_{1-x}As$, we chose a thickness change of $\pm d=5.46$ Å in the barriers and well. Obviously, at one extreme situation, the barrier is narrowed at both ends, while the well is widened at both ends. In another case, the barrier is widened at both ends, and the well is narrowed at both ends. For the sample of present interest, we then have three different situations: (a) 74.08-Å barrier/66.92-Å well/74.08-Å barrier; (b) 85-Å barrier/56-Å well/85-Å barrier; (c) 95.92-Å barrier/45.08- Å well/95.92-Å barrier.

At zero bias, the transmission coefficient $T(E)$ as a function of incident electron energy E is calculated and shown in Fig. 2 for the above three situations. It is clearly indicated in Fig. 2 that the decrease of the barrier width red shifts the resonant state and increases its energy width. The $T(E)$ is also largely increased by decreasing the barrier width. It is found by detailed calculations that the change of the well width also changes the position and the width of the resonant state, but the effect is

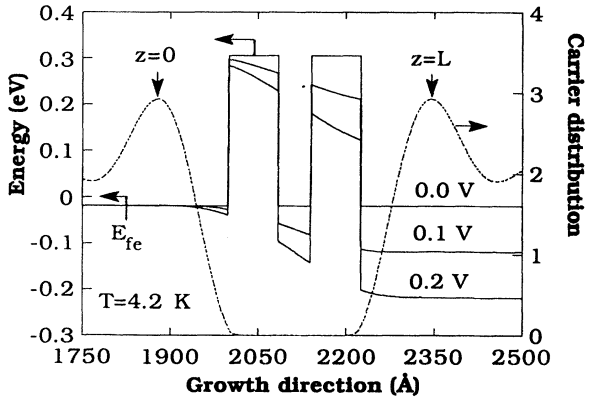

FIG. 1. Band diagrams (solid lines, 0.0-, 0.1-, and 0.2-V bias) and carrier distribution (dotted line, $\times10^{17}$ cm^{-3}) at thermal equilibrium, calculated at $T=4.2$ K. The $z=0$ and L are where the electrons are emitted and collected, respectively. E_{fe} is the quasi-Fermi level position in the emitter region.

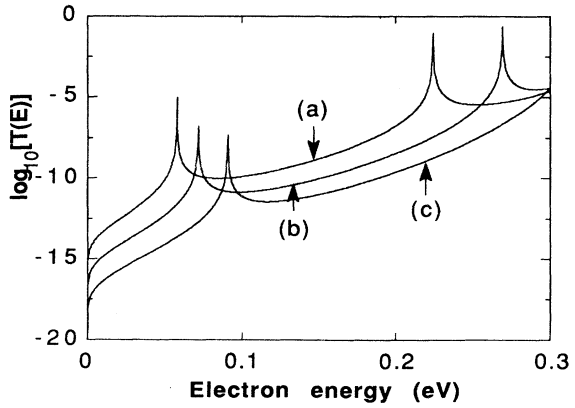

FIG. 2. Tunneling probability $T(E)$ as a function of incident electron energy at zero bias. (a) 74.08-Å barrier/66.92-Å well/74.08-Å barrier; (b) 85-Å barrier/56-Å well/85-Å barrier; (c) 95.92-Å barrier/45.08-Å well/95.92-Å barrier.

smaller than that caused by the barrier width change when the well width is larger (>50 Å). Figure 2 is obtained at zero bias, but remains qualitatively correct with bias.

When one resonant state in the well is biased between $E_c(0)$ and $E_f(0)$, there will be a strong resonant tunneling current. It can be seen from Eq. (3) that when $eV_{ex} > E_f(0) - E_c(0)$, the electronic state in the collector is always available to accept electron tunneling through DBRTS. Since the energy width Δ of the first resonant state is much smaller than 18 meV in the present sample, the tunneling current density is proportional to Δ. As the energy position and Δ of the resonant state are largely influenced by the barrier and well widths, the tunneling current is expected to change substantially by the barrier and well width changes.

The quantitative results are shown in Fig. 3. By changing the barrier width (± 10.92 Å), the current density is changed by a factor of 3. Since the energy position of the resonant state is influenced by the barrier and well widths, the current peak position is also changed (± 35 meV). The energy position change of the resonant state is magnified in the I-V spectrum due to the fact that the external voltage is not only dropped in the well region but in the barrier as well.

The above calculations in Figs. 2 and 3 assume the changes of barrier and well widths at both ends at the same lateral position. In reality, the probabilities of such events are small compared with those of $\pm d$ changes in one of the barriers or the well at one end at one lateral position. By the same calculation scheme, it is easy to show that the effect of only $\pm d$ change in the barrier plus well region is almost a linear extrapolation of the two extreme cases in Figs. 2 and 3.

The probability of lateral nonuniformity is greatly reduced by the improvement of sample growth techniques, but the degree of such lateral nonuniformity (i.e., band-edge discontinuity fluctuation) is intimately tied to the underlying differences in the kinetics of species involved in the materials and cannot be completely avoided. Also, if the sample area is increased, a systematic deviation from the intended interface can easily occur. Since this lateral nonuniformity effect on the I-V spectrum is very significant, it should be detectable even if its probability is rather small. In that case, precaution should be emphasized in interpreting the physical mechanism of the appearance of the fine structures close to the principal tunneling peak in the experimental I-V spectra. For example, the fine structure observed in the valley region of the I-V spectrum in a $Ga_{1-x}Al_xAs/GaAs$ DBRTS (Ref. 12) can also be attributed as a lateral nonuniformity effect, as well as the LO-phonon-emission-assisted tunneling, since the energy shift due to the lateral nonuniformity is also about 30–40 meV and the fine-structure intensity can be matched by a proper consideration of the probability of lateral nonuniformity.

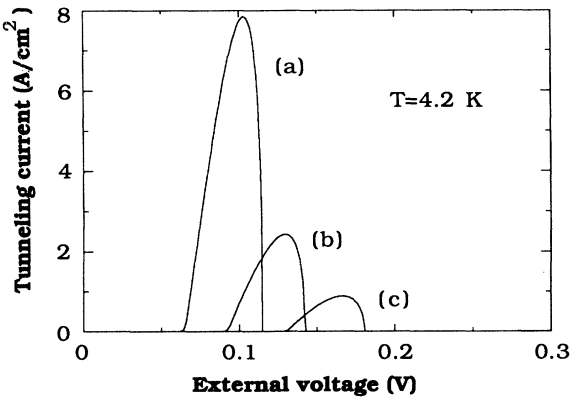

FIG. 3. The effective of ± 10.86-Å change in barrier and well widths on I-V spectra. (a) 74.08-Å barrier/66.92-Å well/74.08-Å barrier; (b) 85-Å barrier/56-Å well/85-Å barrier; (c) 95.92-Å barrier/45.08-Å well/95.92-Å barrier.

Another direct effect of the lateral nonuniformity on the I-V spectrum is the reduction of the peak-to-valley ratio. In Fig. 3, the valley current is still zero at higher voltages (above the 95.86/45.14/95.86 peak in Fig. 3), so its peak-to-valley ratio is unchanged. In reality, the current does not solely come from the tunneling process, so that a background current always exists, which in general increases with increasing voltage. Thus the lateral nonuniformity will increase the valley current, and the peak-to-valley ratio is reduced. One way to minimize such an effect is to increase the well width so that the energy positions of resonant states are lowered. In this way, the first tunneling peak occurs at lower external voltage where the background current is small. The barrier width can also be decreased so that the energy position shifts are reduced for resonant states due to the lateral nonuniformity, and the tunneling peak position changes are reduced in the I-V spectrum. In this way, the tunneling peak width in the I-V spectrum can be kept very narrow, even the degree of lateral nonuniformity and its effect are large. But the increase of the well width will decrease the energy width of the resonant state, which in turn decreases the current density. Therefore, the proper design of the device depends much on its application.

The difference of the first tunneling peak position in the calculated I-V spectrum (Fig. 3) and experimental data[6] can be understood as a result of the drop of the external voltage on another region of the sample. The carrier accumulation effect here is small due to the fact that the current intensity is small when tunneling through the first resonant state in the well.

In a brief summary, we report here the lateral nonuniformity effect on the I-V spectrum in DBRTS. It is shown that the change of two atomic layers (an anion layer and a cation layer) in the barrier plus well region will have a substantial effect on the I-V spectrum. Such an effect can be a possible cause of the fine structures in the I-V spectrum. Since the lateral nonuniformity is hardly avoided, its influence on the I-V spectrum should be included in the proper consideration for the physical interpretation of experimental data and the device design for application.

This work was financially supported by the Swedish Natural Science Research Council.

[1]B. Ricco and M. Y. Azbel, Phys. Rev. B **29**, 1970 (1984).
[2]S. Luryi, Appl. Phys. Lett. **47**, 490 (1985).
[3]H. Morkoç, J. Chen, U. K. Reddy, T. Henderson, and S. Luryi, Appl. Phys. Lett. **49**, 70 (1986).
[4]H. Ohnishi, T. Inata, S. Muto, N. Yokoyama, and S. Shibatomi, Appl. Phys. Lett. **49**, 1248 (1986).
[5]V. J. Goldman, D. C. Tsui, and J. E. Cunningham, Phys. Rev. B **35**, 9387 (1987).
[6]V. J. Goldman, D. C. Tsui, and J. E. Cunningham, Phys. Rev. Lett. **58**, 1256 (1987).
[7]J. O. Sofo and C. A. Balseiro, Phys. Rev. B **42**, 7292 (1990).
[8]N. C. Kluksdahl, A. M. Kriman, D. K. Ferry, and C. Ringhofer, Phys. Rev. B **39**, 7720 (1989).
[9]A. Madhukar, in *Physics of Quantum Electron Devices,* edited by F. Capasso (Springer-Verlag, Berlin, 1990), p. 50.
[10]R. Dingle, R. A. Logan, and J. R. Arthur, Jr., in *International Symposium on Gallium Arsenide and Related Compounds,* edited by C. Hilsum, IOP Conf. Proc. No. 33A (Institute of Physics and Physical Society, London, 1977), p. 210.
[11]S. Adachi, J. Apply. Phys. **58**, R1 (1985).
[12]V. J. Goldman, D. C. Tsui, and J. E. Cunningham, Phys. Rev. B **36**, 7635 (1987).